Title: Transit Timing and Duration Variations for the Discovery and Characterization of Exoplanets

Eric Agol and Daniel C. Fabrycky

Abstract Transiting exoplanets in multi-planet systems have non-Keplerian orbits which can cause the times and durations of transits to vary. We review the theory and observations of transit timing variations (TTV) and transit duration variations (TDV).

Introduction

Transit Timing Variations (TTV) and Transit Duration Variations (TDV) are two of the newest tools in the exoplanetary observer's toolbox for discovering and characterizing planetary systems. Like most such tools, they are indirect inferences. However, the amount of dynamical information they encode is extremely rich.

To decode this information, let us start with the dynamical concepts. Consider the vector stretching from the star of mass $M_\star$ to the planet of mass M_p to be $\mathbf{r} = (x, y, z)$, with a distance r and direction $\hat{\mathbf{r}}$. The Keplerian potential, $\phi = -GM/r$ (where $M \equiv M_\star + M_p$ and the planet is replaced with a body of reduced mass $\mu \equiv M_\star M_p/(M_\star + M_p)$), is one of only two radial, power-law potentials that gives rise to closed orbits [1]. This means that, in the absense of perturbations, there is a strict periodicity $\mathbf{r}(t+P) = \mathbf{r}(t)$. Moreover, Kepler showed that Tycho Brahe's excellent data for planetary positions were consistent with Copernicus' idea of a heliocentric system only if the planets (including the Earth) followed elliptical paths of

Eric Agol
Department of Astronomy, Box 351580, University of Washington, Seattle, WA 98195-1580, USA
e-mail: agol@uw.edu

Daniel C. Fabrycky
Dept. of Astronomy & Astrophysics, University of Chicago, Chicago, IL 60637, USA e-mail: fabrycky@uchicago.edu

[1] the other one, the harmonic potential $-kr$ would only have relevance for collisionless orbits within a homogeneous massive body

semi-major axis a, and one focus on the Sun. Newton was successful at finding the principle underlying such orbits, a force law $\mathbf{F} = \mu\ddot{\mathbf{r}} = -G\mu M r^{-2}\hat{\mathbf{r}}$, which results in a period $P = 2\pi a^{3/2}G^{-1/2}(M_\star + M_p)^{-1/2}$ (i.e. with the a-scaling Kepler found the planets actually obeyed).

This research program was thrown into some doubt by the "Great Inequality," the fact that the orbits of Jupiter and Saturn did not fit the fixed Keplerian ellipse model. This was overcome by the perturbation theory of Laplace, who used the masses derived via their satellite orbits to explain their deviations of their solar orbits (Wilson 1985). We can recreate the main effect of this insight by writing an additional force to that of gravity of the Sun:

$$\mathbf{F_1} = -G\mu_1 M r_1^{-2}\hat{\mathbf{r}}_\mathbf{1} + \mathbf{F_{21}}, \tag{1}$$

where we now specify forces and distances explicitly to planet 1, and add a force of planet 2 on planet 1. This latter force consists of two terms:

$$\mathbf{F_{21}} = \mu_1\ddot{\mathbf{r}}_\mathbf{1} = -G\mu_1 M_2|r_1 - r_2|^{-3}(\mathbf{r_2} - \mathbf{r_1}) + G\mu_1 M_2 r_2^{-2}\hat{\mathbf{r}}_\mathbf{2}. \tag{2}$$

The first term on the right-hand-side is the direct gravitational acceleration of planet 1 due to planet 2. The second is a frame-acceleration effect, due to the acceleration the Sun feels due to the second planet. Since the Sun is fixed at the zero of the frame, this acceleration is manifested by acceleration in the opposite direction of planet 1.

Likewise, Leverrier and Adams used the same technique, dynamical perturbations, to discover the first planet by gravitational means (Adams 1847; Le Verrier 1877). In this case, they did not know the zeroth order solution (i.e. the Keplerian ellipse) for the yet-to-be-discovered Neptune. In its place, they assumed the Titius-Bode rule held, and sought only the phase of the orbit. This worked because they only wanted to see how the acceleration, then deceleration, as Uranus passed Neptune, would betray its position on the sky to optical observers. [Say later: the task that researchers set for themselves to discover planets by TTV is a bit more demanding. We do not have any hints as to what the planet's orbit might be (neither circular nor roughly obeying some spacing law). Additionally, the data per orbit is considerably noisy; in only a few cases are the orbit-by-orbit "chopping" signal statistically significant after just three transits. Finally, the orbit is only sampled at the transit phase, so opportunities for aliasing of the signal are abundant.]

The discovery of transits marks the first time that data on exoplanets could be precise enough to notice gravitational interactions.[2] The times of transit are primarily constrained by the decline of stellar flux during transit ingress, and the rise over egress, which occur on a timescale

$$\tau \approx \pi^{-1}P(R_p/a) \approx 10^{-4}P\left(\frac{3R_p}{R_\oplus}\right)\left(\frac{a}{0.3\mathrm{AU}}\right)^{-1}, \tag{3}$$

[2] Only around the same time (2000) were perturbations noticed in the resonant interaction of the planets of GJ 876 (Laughlin and Chambers 2001).

assuming an impact parameter of $b = 0$. This allows the transit times to be measured precisely relative to the orbital period, giving a sensitive measure of the variation of the angular position of a planet relative to a Keplerian orbit. In contrast, the stellar radial velocity varies on the orbital timescale, and thus the precision of the orbital phase is poorly constrained unless the measurements are of high precision or long duration (which allows deviations to grow with time).

We may define express the orbital positions or transit times in a table called an ephemeris, and the perturbations cause motions or timing deviations from a Keplerian reference model. In the case of transit timing variations, the Keplerian alternative is simply an ephemeris with a constant transit period, P:

$$C = T_0 + P \times E, \tag{4}$$

where E is the integer number of a transit and T_0 is the time of the first transit; C stands for "calculated" based on a constant-period model. Meanwhile, the Observed times of transit are denoted O. This notation leads to an "O minus C" diagram, in which only the perturbation part is plotted. An instructive version, modelled after the timing of WASP-47 (Becker et al 2015) but with a greatly exaggerated perturbation, is shown in figure 1. The transit times come earlier than the linear model for transit numbers 0-3 and 10-14, and later than the linear model for transit numbers 4-9. This correlated residual structure is what we call TTVs.

The other dynamical effect addressed by this review is TDVs. Like TTVs, the cause can be changes in the orbit period or eccentricity. The most dramatic effect, however, is due to orbital plane reorientation. The angle the orbit's normal vector makes to the observer's line of sight — the inclination — determines the length of the transit chord. Changes in the inclination will change the length of that chord, which in turn changes the amount of time the planet remains in transit.

The literature on exoplanets has a history of rediscovering effects that had been well studied in the field of binary and multiple stars. In the current focus, it has long been known to eclipsing-binary observers that long-term depth changes can result from the torque of a third star orbiting the pair (Mayer 1971). Its exoplanetary analogue is transit duration variation (TDV) due to perturbing planets (Miralda-Escudé 2002). This effect owes to the secular and tidal dynamics which dominate triple star systems (Borkovits et al 2003), dictated by their hierarchical configuration which allows them to remain stable. Planetary systems can be much more compact due to the dominant mass of the central star, and so mean-motion resonances can dominate their dynamics. TTVs due to mean-motion resonances is thus a novel aspect of exoplanet systems.

The first recognition of the importance of transit timing and duration variations was at the DPS and AAS meetings two decades ago by Dobrovolskis and Borucki (1996a,b), followed a few years later by Miralda-Escudé (2002) and Schneider (2003, 2004). More detailed studies which included the important effect of mean-motion resonance were submitted simultaneously by Holman and Murray (2005) and Agol et al (2005). The former paper showed that Solar-system like perturbations might be used to find Earth-like planets, should transit times be measured with

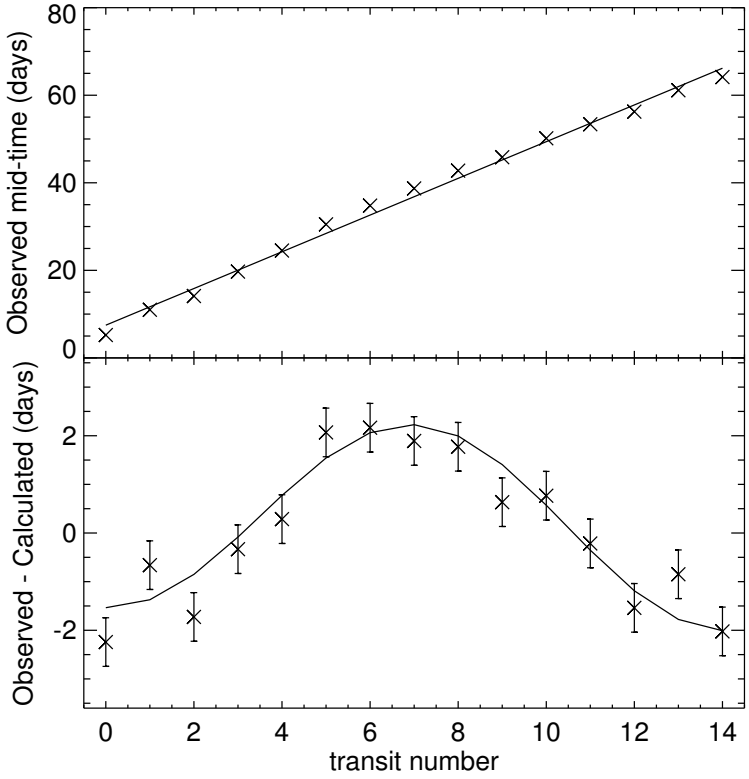

Fig. 1 An example of timing data. *T*op panel: the measured midtimes of exoplanet transits, to which a line is fit by least-squares. *B*ottom panel: the residuals of that fit, which is the conventional $O-C$ diagram; the original sinusoidal function, to which Gaussian noise was added, is also plotted as a line.

sufficient accuracy. The latter paper coined the term 'transit-timing variations,' with acronym TTV, and defined TTVs as being the residuals of a linear fit to the times of a transiting planet.

Initial studies of TTVs of hot Jupiters were able to place limits on the presence of Earth-mass planets near mean-motion resonance. Some further studies claimed detection of perturbing planets causing TTVs or TDVs, but each of these were quickly disputed or refuted by additional measurements. The first convincing detection awaited the launch of the Kepler spacecraft, and the detection of Kepler-9 which showed large-amplitude TTVs of two Saturn-sized planets with strong significance (Holman et al 2010); this discovery was remarkably similar to predictions that had been made based upon the GJ 876 system (Agol et al 2005). This paper kicked off a series of discoveries of TTVs with the Kepler spacecraft, with now more than 100 systems displaying TTVs, and a handful showing TDVs.

Preliminaries

Since the gravitational interactions between planets occurs on the orbital timescale, the amplitude of transit timing variations is proportional to the orbital period of each planet, as well as a function of other dimensionless quantities. Thanks to Newton's second law and Newton's law of gravity, the acceleration of a body does not depend on its own mass. Thus, the transit timing variations of each planet scale with the masses of the *other* bodies in the system. In a two-planet system, then, to lowest order in mass ratio,

$$|\delta t_1| = \frac{P_1}{2\pi}\frac{m_2}{m_0} f_{12}(\alpha_{12}, \theta_{12}),$$
$$|\delta t_2| = \frac{P_2}{2\pi}\frac{m_1}{m_0} f_{21}(\alpha_{12}, \theta_{21}), \tag{5}$$

where the masses of the star and planets are m_0, m_1, and m_2, and f_{ij} governs the timing variations of planet j on planet i, which is a function of the semi-major axis ratio, $\alpha_{12} = a_1/a_2 < 1$, and the angular orbital elements of the planets, $\theta_{ij} = (\lambda_i, \omega_i, I_i, \Omega_i, \lambda_j, \omega_j, I_j, \Omega_j)$.

For the largest TTVs, those caused by orbital period changes associated with librations of the system about a mean-motion resonance, we may appeal to energy trades to compute the amplitude of the TTV in each planet (see Holman et al 2010). A period lengthening of $\delta t_1 \ll P_1$ is associated with a semi-major axis change of $\delta a_1 = (3/2) a_1 \delta t_1 / P_1$, because of Kepler's relation $a \propto P^{3/2}$. Differentiating the orbital energy equation $E_1 = -GMm_1/(2a_1)$ shows that such a change results in an energy change of $\delta E_1 = (GMm_1 a_1^{-2}/2)\delta a_1$. To conserve total energy, the other planet will have an energy change of $E_2 = -(GMm_1 a_1^{-2}/2)\delta a_1$, which can also be expressed as $+(GMm_2 a_2^{-2}/2)\delta a_2$. Using the relation $\delta a_2 = (3/2) a_2 \delta t_2 / P_2$, and the Keplerian relation $a_2/a_1 = (P_2/P_1)^{2/3}$, we obtain:

$$\delta t_2 = -\delta t_1 (m_1/m_2)(P_2/P_1)^{5/3}. \tag{6}$$

Hence the TTV curves of the two planets are anti-correlated, and the amplitude of the outer planet's TTV is considerably larger to compensate for the smaller amount that its Keplerian orbital energy contributes to the interaction.

With the addition of multiple perturbing planets, if the mass-ratios of the planets to the star is sufficiently small and if none of the planets exist in a resonant configuration, then the transiting timing variations may be approximately expressed as linear combinations of the perturbations due to each companion. For N planets, the TTVs become

$$\delta t_j = P_j \sum_{i \neq j} \frac{m_i}{m_0} f_{ij}(\alpha_{ij}, \theta_{ij}). \tag{7}$$

Note that $\alpha_{ij} = \min(a_i/a_j, a_j/a_i)$.

The measurement of TTVs and TDVs has been used for confirmation, detection, and characterization of transiting exoplanets and their companions. The Ke-

pler spacecraft discovered thousands of transiting exoplanet candidates; the classification as 'candidate' was cautiously used to allow for other possible explanations, such as a blend of a foreground star and a background eclipsing binary causing an apparent transit-like signal. The presence of multiple transiting planets around the same star gave a means of confirming two planets that display *anti-correlated* TTVs: due to energy and angular momentum conservation, the anti-correlation indicates dynamical interactions between the two planets, while such a configuration would not be stable for a triple star system. A series of papers used this technique to confirm that Kepler planet candidates were bonafide exoplanets: Ford et al (2011, 2012a); Fabrycky et al (2012); Ford et al (2012b); Steffen et al (2012, 2013); Xie (2013, 2014).

The confident detection of perturbing exoplanets with TTVs awaited the Kepler spacecraft as well. The Kepler-19b planet showed sinusoidal TTVs that were used to identify a handful of possible planet period and mass combinations that might be responsible for the perturbations (Ballard et al 2011). The unique identification of a perturbing planet was accomplished with Kepler-46 (aka KOI-872) which displayed very high signal-to-noise TTVs which allowed the period and mass of the perturber to be measured with some precision (Nesvorný et al 2012). The detection and characterization of a perturbing planet in KOI-142 required both TTV and TDV (Nesvorný et al 2013).

The characterization of exoplanets with TTVs also began in earnest with the Kepler spacecraft. In addition to Kepler-9, the Kepler-18 system was characterized by a combination of TTVs and RVs, giving density estimates for the three transiting planets (Cochran et al 2011).

The characterization of exoplanets is complicated by degeneracy between mass and eccentricity caused by aliasing at the frequency of the transiting planet (discussed below). However, in general transit timing variations gives a means of measuring the density of exoplanets. The two observables associated with a light curve are the time stamp of each photometric measurement and the number of photons measured. The number of photons is a dimensionless number, and thus may only constrain dimensionless quantities, such as radius ratio, impact parameter, or the ratio of the stellar size to the semi-major axis. The quantities that have units of time — the period, transit duration, ingress duration — can further constrain the density of the system since the dynamical time $t_{dyn} \approx (G\rho)^{-1/2}$. Seager and Mallén-Ornelas (2003) showed that a single transiting planet on a well-measured circular orbit may be used to gauge the density of the star; in the case of multiple transiting planets, the circular assumption may be relaxed (Kipping 2014). The transit depth, then, gives the radius-ratio of the planet to the star, while if two transit and show TTVs, their TTVs give an estimate of the mass ratio of their perturber to the star. Thus, two transiting, interacting planets yield an estimate of the density ratio of the planets to the star, and consequently we can obtain the density of the planets. Note that this is true even if the absolute mass and radius of the star are poorly constrained. A caveat to this technique is that there is an eccentricity dependence that is present in TTVs as well, but typically multi-transiting planet systems require low eccentricities to be stable, and in some cases the eccentricities can be constrained sufficiently

from TTVs, from analyzing multiple planets (Kipping 2014), or statistically from an ensemble analysis (Hadden and Lithwick 2014), so this ends up not impacting the stellar density estimate significantly, although it can impact the planet-star mass ratios, and hence inflate the planet density uncertainty. Another way to obtain an estimate of stellar density is from asteroseismology: in fact, the time dependence of asteroseismic measurements is what enables density to be constrained in that case as well (Ulrich 1986).

If a pair of transiting exoplanets can be detected with *both* TTVs and RVs, then the absolute dimensions of the system can be obtained (Agol et al 2005; Montet and Johnson 2013) as RVs have a dimensions of velocity, which when combined with time measurements from TTVs gives dimensions of distance. In practice this technique has yet to yield useful constraints upon the properties of planetary systems (Almenara et al 2015), but it may prove fruitful in the future much as double-lined spectroscopic binaries have used to measuring the properties of binary stars. Circumbinary planets (CBP) are an extreme example of this technique: the timing offsets of the transits, combined with the eclipses and radial-velocity of the binary give very precise constraints on the absolute parameters of the Kepler-16 system (Doyle et al 2011).

Theory

Here we discuss the physical models for different types of TTV interactions, and point the reader to real systems that exhibit that kind of interaction.

In the hierarchical case, in which the outer planet transits, and the inner orbiting body is very massive, the dominant effect can be the shifting of the primary star with respect to the barycenter. Then, as the outer planet orbits the barycenter, it arrives at the moving target either early or late. This effect was numbered (i) by Agol et al (2005), and it is seen clearly in circumbinary planet systems. For instance, the secondary star in of Kepler-16 (Doyle et al 2011) moves the primary by many times its own radius, resulting in an ~ 8 day TTV on top of a 225 day orbit. [DF]

Close to resonances, a combination of changes in semi-major axis and eccentricity lead to TTV cycles whose period depends on the separation from the resonance and the amplitude depends on the masses and eccentricites (Lithwick et al 2012). The main TTV variation comes from only one resonance, the one the system is closest to, which allows its critical angles to move slowly and thus its effect to build up. If the period ratio P_2/P_1 is within a few percent of a j/k, with j and k being integers, then the expected TTV frequency is $|j/P_2 - k/P_1|$, the TTV period being the reciprocal of that expression. The order of the resonance is $|j-k|$, and the strength of the resonance depends on the planetary eccentricities to a power of the order minus 1. Therefore, first order resonances affect planets with no initial eccentricity, but higher order resonances have a large effect only in the presence of some eccentricity.

Seeing two planets transit the star helps immensely in characterization of a near-resonant system, because then the relative phase of the two planets can be compared

with the phase of the TTV (Lithwick et al 2012). If the eccentricities are maximally damped out, then the resonant terms of the interaction continue forcing a small eccentricity that quickly precesses, causing the TTV. In that case, the phase of the signal is predictable, and the planetary eccentricities are anti-aligned, so the TTV in the two planets consists of anti-corrlated sinusoids. Also useful in that case: the amplitudes lead directly to the planetary masses. If so-called "free eccentricity" remains, however, the phases would naturally differ from that prediction, the variations in the two planets may be somewhat out of phase from each other, and only an approximate mass scale rather than a measurement is available. The first real system that showed this pattern convincingly was Kepler-18 (Cochran et al 2011) [figure of that rather than the theory one given currently in figure 2?].

When only one planet transits in a near-resonant system, the measured TTVs may simply record a sinusoidal signal, which could result from the other planet being close to many different resonances with the transiting planet. In Kepler-19, Ballard et al (2011) were able to tell that a planetary companion was the only sensible cause of the TTV, bu they were not able to break this finite set of degeneracies.

This degeneracy has made it extremely difficult to characterize non-transiting planets via TTV, and hence in many cases an additional planet is suspected due to TTV, but detailed work is not pursued to show its nature. The first case of a non-transiting planet being discovered *and* completely characterized was Kepler-47 (a.k.a. KOI-872; Nesvorný et al 2012). The authors found that the TTVs of the transiting planet were far from a sinusoidal shape; in fact, they could be fourier-decomposed into at least four significant sinusoids. Each of these sinusoids can be identified as the interaction with the non-transiting planet via a different resonace. Even with all this extra information, TTVs could only narrow down the possible second planets to a degenerate set of two planets. The clever solution (Nesvorný et al 2012) was to note that one of those solutions, to get the relative amplitudes of the various sinusoids correct, would require the perturbing planet to be somewhat inclined with respect to the transiting planet. As a consequence, a torque on that planet would drive TDV. No such TDV were observed, so the unique solution was found.

Planets that are truly in resonance with each other have the largest TTV signals. On a medium-baseline timescale like that of Kepler, they can perturb each other's orbital periods. The resonant interaction traps the planets at a specific period ratio, causing the periods to oscillate near that ratio. The period of the full cycle of that oscillation depends on the ratio of the planet masses to the host star's mass, to the $-2/3$ power (Nesvorný and Vokrouhlický 2016). For instance, the touchstone system GJ876 has a 550 day libration cycle, about 10 times the outer planet's period, due to its relatively massive planets and low-mass star. A system which was characterized by resonant interaction is KOI-142 (Nesvorný et al 2013), in which a non-transiting planet was discoverd. A system with two transiting planets in resonance with large TTVs is Kepler-30 (Fabrycky et al 2012). A system with smaller libration amplitudes, but a surprising *four* planets in resonance (forming a chain of resonances) is Kepler-223 (Mills et al 2016).

Chopping

When two planets are nearly resonant, the degeneracy between the mass ratios of the planets to the star and the eccentricity vector may be broken by examining additional non-resonant harmonics present in the data (Deck and Agol 2015). These additional harmonics have a smaller amplitude due to the fact that they are not caused by resonant terms, and thus require higher signal-to-noise to break the degeneracy between the mass and eccentricity. Nevertheless, the chopping component can be detected in many cases, and leads to a unique measurement of the masses of the exoplanets (Nesvorný and Vokrouhlický 2014; Schmitt et al 2014; Deck and Agol 2015).

As an example, consider a pair of planets with period ratio of $P_2/P_1 = 1.52$. This period ratio is close to 3:2, and thus is affected by this resonant term, giving a TTV period of $75P_1$. Figure 2 compares two planets with this period ratio with zero eccentricity and mass-ratios of 10^{-6} to a pair of planets with eccentricites of $e_1 = e_2 = 0.04$ and mass-ratios near 10^{-7}. Both pairs of planets give nearly identical amplitudes for the resonant term, while the larger mass ratio planets show a much stronger chopping variation. In this case there is a clear difference between the TTVs of the two simulated systems: the inner planet shows a drift over three orbital periods, and a sudden jump every third orbital period, while the outer one shows a similar pattern over two orbital periods. These variations are due to perturbations at integer multiples of the synodic frequency, which has a period $P_{syn}^{-1} = 1/P_1 - 1/P_2$. In this example we have set the phase of the orbital parameters to be such that the TTVs match; change in the phase can also be indicative of a non-zero eccentricity contributing to the TTVs, and with an ensemble of planets which are believed to have a similar eccentricity distribution, the mass-eccentricity degeneracy may be broken statistically (Lithwick et al 2012; Hadden and Lithwick 2014).

- Exomoons [EA] - Light time? Borkovits deconvolution [DF] - Borkovits(?) - KOI 1474 cleaner example? Or leave out? Future – circumstellar planets in binaries; Schwartz et al. w/ Haghighipour. [DF] - TDVs

Observations/Practical considerations

Confirmation of multi-planet systems in Kepler anti-correlated sinusoids, Ford GPs [DF] –¿ mentioned above

Transit Duration Variations

Compared with TTVs, TDVs have shown relatively few results.

The most dramatic TDVs are due to the moving-target effect described for TTVs in the context of CBPs. For instance, it was discussed extensively by Kostov et al (2013) for the cases of Kepler-47 and of KIC 4862625b (a.k.a. PH-1).

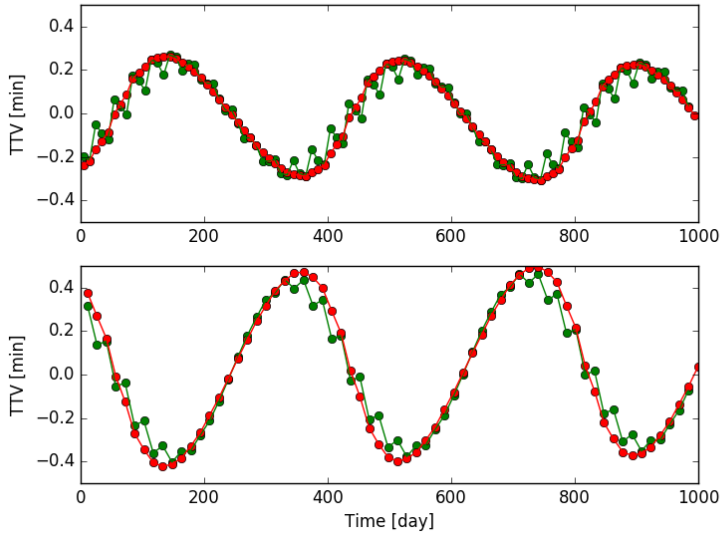

Fig. 2 Transit-timing variations of two low-eccentricity planets with larger mass ratios, $m_1 = m_2 = 10^{-6} m_*$ (green) compared with two higher eccentricity planets ($e_1 = e_2 = 0.04$) with smaller mass ratios $m_1 = m_2 = 10^{-7} m_*$. The zig-zag chopping component is apparent in the high-mass/low-eccentricity case, while less apparent in the low-mass/ high-eccentricity case.

Following the cases of stellar triples, the precession of CBPs has caused transits to turn on and off (Martin 2017). The first case of that phenomenon was Kepler-35 (Welsh et al 2012), and the most spectacular so far observed was Kepler-413 (Kostov et al 2014).

In planetary system orbiting a single primary, there are three mechanisms that have caused TDV to be observed.

The first is just the planetary torques due to mutual inclination. This was observed in Kepler-117 (Almenara et al 2015) as well as Kepler-108 (Mills and Fabrycky 2017), the latter indicating mutual inclination of $\sim 15^\circ$ in a rather hierarchical pair of planets.

The second mechanism for TDV in planetary systems is torques not due to another planet, but due to the rotational oblateness of the star. It is a convincing model for the duration changes in KOI-13 (Almenara et al 2015) and a controversial explanation for transit shape anomalies in PTFO 8-8695 (Barnes et al 2013).

A final planetary cause of TDVs is dramatic eccentricity variations due to a resonant interaction. The length of the chord across the star, as well as the speed at which the planet moves along that chord, are changed during the planetary interaction. This effect has been observed in KOI-142 (Nesvorný et al 2013). - Precession - Kepler-108 1606.04485 / KOI-142 Nesvorny / KOI-13 (Mazeh) - and CBPs turning on or off. [DF]

Finally, it has not been measured yet, but slow secular precession of the eccentricity is expected by general relativity (Pál and Kocsis 2008), by stellar oblateness (Heyl and Gladman 2007), and by tidal distortion (Ragozzine and Wolf 2009). It is likely that very long time-baseline measurements, or comparing the measurements of two time-separated space missions like Kepler and Plato, will be able to detect this.

Timing precision

The steepest portions of a transit are the ingress and egress when the planet crosses onto and off of the disk of the star, causing a dip of depth $\delta = (R_p/R_*)^2$ if we ignore limb-darkening. Suppose for the moment that the only source of noise is Poisson noise due to the count rate of the star, $\dot{N}$. The photometric precision over the duration of ingress scales as $(\dot{N}\tau)^{1/2}$, where τ is the ingress duration (eqn. 3). If the time of ingress fit from a model is offset by σ_g, then the difference in counts observed versus the model is $\sigma_g \delta \dot{N}$ (the pink region in Fig. 3). Equating this to photometric uncertainty gives $\sigma_g = \tau^{1/2}\dot{N}^{-1/2}\delta^{-1}$, which is the 68.3% confidence timing precision assuming that the exposure time is much shorter than the ingress duration and that $\sigma_g \ll \tau$. The same formula applies to egress. A longer transit ingress duration leads to a shallower slope in ingress, which makes it more difficult to measure an offset in time of the model. Higher count rates and deeper transits improve the precision, as expected. Note that we've assumed that the duration of the transit is sufficiently long that the error on δ is small.

Suppose the transit duration is T. Then, the uncertainty on the duration is given by the sum of the uncertainties on the ingress and egress, added in quadrature: $\sigma_T = \sqrt{2}\sigma_g$. The timing precision, σ_t, is set by the mean of the ingress and egress, giving $\sigma_t = \frac{1}{\sqrt{2}}\sigma_g$.

A more complete derivation of these expressions is given by Carter et al (2008), while an expression which includes the effects of a finite integration time is given by Price and Rogers (2014). The assumptions of no limb-darkening and Poisson noise are generally broken by stars; in addition, stellar variability contributes to timing uncertainty, for which there is yet to be a general expression. These effects generally increase the uncertainty on the measurement of transit times and durations, and so the best practice would be to estimate the timing uncertainties from the data, accounting for effects of correlated stellar variability by including the full covariance matrix of the timing uncertainty (Carter and Winn 2009; Gibson et al 2012). Crossing of the path of the planet across star spots may also cause some uncertainty on the timing precision; this can be diagnosed by a larger scatter within transit than outside transit or other signs of significant stellar activity, and can be handled best by including the spots in the transit model Ioannidis et al (2016).

Note that the barycentric light-travel time offset must be corrected for carefully for high-precision TTV (Eastman et al 2010).

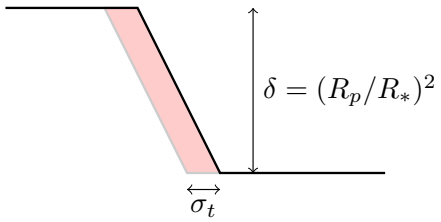

Fig. 3 Diagram of the transit ingress of a planet. The precision of the timing of ingress, σ_g, is set by when the area of the ingress (pink) equals the timing precision over the duration of ingress.

Science Results

The best characterized pair of planets to date using TTV reside in the Kepler-36 system (Carter et al 2012). As this planet pair is close to a 6:7 period ratio, the conjunctions cause a significant kick to each planet resulting a TTV amplitude that is $\approx 1\%$ of the orbital periods of the planets. Figure 4 shows a 'river-plot' for all seventeen quarters of long-cadence Kepler data for this pair of planets. After each 7(6) orbits of the inner(outer) planet, there is a conjunction which causes a change in the eccentricity vector and period of each planet. The change in the eccentricity vector causes a sudden change in the subsequent transit time, while the change in period causes a change in slope; these are apparent for Kepler-36c in Figure 4. The large TTVs enable a precise measurement of the planet-star mass ratios for both planets (using the TTVs of the companion planet), while the star shows asteroseismic variability which gives precise planets for the stellar mass. The net result are masses with uncertainties of $< 8\%$, which is precise for planets of this size. The inner planet shows a density which is consistent with scaling up the composition of Earth, while the outer planet requires a significant H/He envelope to explain its size which is comparable to Neptune (Carter et al 2012).

- Other favorite systems? Kepler-11 puffy/packed planets [DF]
- Best eccentricity constraint for a super-Earth? Kepler-36? Include?
- Ensemble TTV analysis: Xie - differing architecture for the single-transiters due to less frequent TTV, Hadden-Lithwick - eccentricity distribution; Hot Jupiters lonely (Steffen); Latham - gas giants less frequent in multi-transiting (no TTVs) [DF]
- Measuring masses - Steffen bias? [DF]
- CBPs [DF]

Catalogs of transit times have been produced for the multi-planet Kepler systems (Mazeh et al 2013; Holczer et al 2016). Several analyses of an ensemble of TTV pairs of planets have recently been carried out (Hadden and Lithwick 2014; Xie 2013, 2014; Jontof-Hutter et al 2016), with the largest by Hadden & Lithwick (2016). With a slightly smaller sample, we have selected only planets with mass precisions of better than $3-\sigma$ in Figure 5. There appears to be a trend of mean density decreasing with orbital period (one exception is K2-3d, although the authors warn its RV mass may be affected by stellar variability). At periods near ≈ 10 days, the

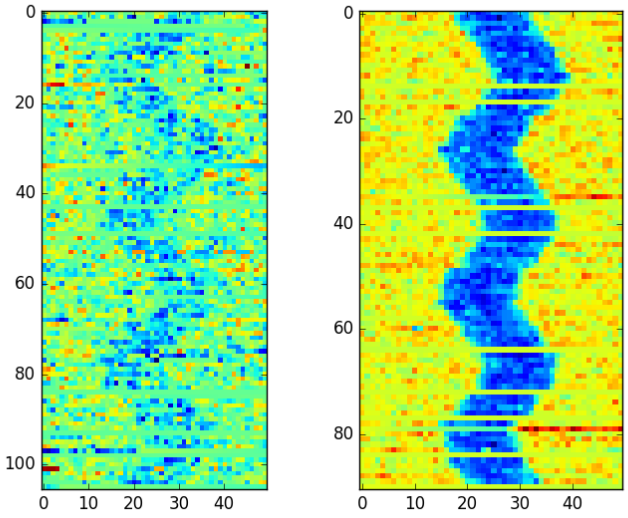

Fig. 4 River plot of Kepler-36b (left) and Kepler-36c (right).

RV and TTV densities agree rather well. At shorter period, most of the RV detections are single-planets, whic in general appear to have lower density relative to their multi-planet counterparts. When radius is plotted versus mass, and color-coded as a function of flux, Fig. 5, there is a general trend radius increasing with mass, albeit with a large scatter in mass, while a handful of of 'puffy' planets (with masses measured with TTV) show absurdly large radii given their small masses. These mass measurements are surprising, but difficult to dispute as larger masses would have led to a larger, and hence easier-to-measure, TTV signal.

Future

- More thorough TTV analysis: GPs - for measuring transit times - Follow-up of Kepler targets - Comparison of TTV masses with RV masses: better constraints and confidence in both methods? - MCMC with high-multiplicity systems - TESS, JWST, CHEOPS, PLATO, ? - TTV/TDV of exomoons - HZ exoplanets - Smaller CBPs - Stellar/planet characterization: TTV + RV

References:

Borucki & Summers Struve Cabrera Charbonneau 2000

Neptune: Bouvard/Adams/Le Verrier/Galle

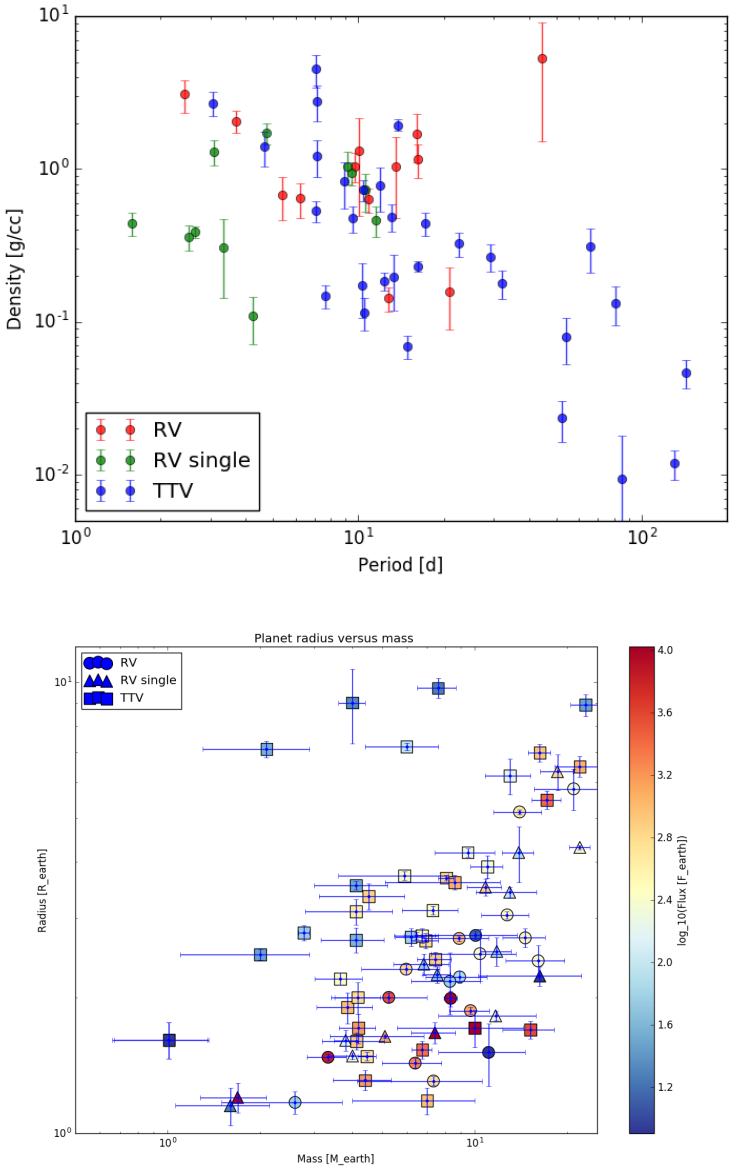

Fig. 5 Density vs. period for planets transiting planets with masses $< 25 M_{\oplus}$ (left). Radius vs. mass, with color indicating incident stellar flux (right).

Acknowledgements EA acknowledges support from NASA Grant ... DCF acknowledges support from NASA KPS-3 grant.

References

Adams JC (1847) An Explanation of the Observed Irregularities in the Motion of Uranus, on the Hypothesis of Disturbances caused by a more Distant Planet; with a Determination of the Mass, Orbit, and Position of the Disturbing Body. MmRAS16:427

Agol E, Steffen J, Sari R Clarkson W (2005) On detecting terrestrial planets with timing of giant planet transits. MNRAS359:567–579, DOI 10.1111/j.1365-2966.2005.08922.x, astro-ph/0412032

Almenara JM, Díaz RF, Mardling R et al (2015) Absolute masses and radii determination in multiplanetary systems without stellar models. MNRAS453:2644–2652, DOI 10.1093/mnras/stv1735, 1508.06596

Ballard S, Fabrycky D, Fressin F et al (2011) The Kepler-19 System: A Transiting 2.2 R $_\oplus$ Planet and a Second Planet Detected via Transit Timing Variations. ApJ743:200, DOI 10.1088/0004-637X/743/2/200, 1109.1561

Barnes JW, van Eyken JC, Jackson BK, Ciardi DR Fortney JJ (2013) Measurement of Spin-orbit Misalignment and Nodal Precession for the Planet around Pre-main-sequence Star PTFO 8-8695 from Gravity Darkening. ApJ774:53, DOI 10.1088/0004-637X/774/1/53, 1308.0629

Becker JC, Vanderburg A, Adams FC, Rappaport SA Schwengeler HM (2015) WASP-47: A Hot Jupiter System with Two Additional Planets Discovered by K2. ApJ812:L18, DOI 10.1088/2041-8205/812/2/L18, 1508.02411

Borkovits T, Érdi B, Forgács-Dajka E Kovács T (2003) On the detectability of long period perturbations in close hierarchical triple stellar systems. A&A398:1091–1102, DOI 10.1051/0004-6361:20021688

Carter JA Winn JN (2009) Parameter Estimation from Time-series Data with Correlated Errors: A Wavelet-based Method and its Application to Transit Light Curves. ApJ704:51–67, DOI 10.1088/0004-637X/704/1/51, 0909.0747

Carter JA, Yee JC, Eastman J, Gaudi BS Winn JN (2008) Analytic Approximations for Transit Light-Curve Observables, Uncertainties, and Covariances. ApJ689:499-512, DOI 10.1086/592321, 0805.0238

Carter JA, Agol E, Chaplin WJ et al (2012) Kepler-36: A Pair of Planets with Neighboring Orbits and Dissimilar Densities. Science 337:556, DOI 10.1126/science.1223269, 1206.4718

Cochran WD, Fabrycky DC, Torres G et al (2011) Kepler-18b, c, and d: A System of Three Planets Confirmed by Transit Timing Variations, Light Curve Validation, Warm-Spitzer Photometry, and Radial Velocity Measurements. ApJS197:7, DOI 10.1088/0067-0049/197/1/7, 1110.0820

Deck KM Agol E (2015) Measurement of Planet Masses with Transit Timing Variations Due to Synodic "Chopping" Effects. ApJ802:116, DOI 10.1088/0004-637X/802/2/116, 1411.0004

Dobrovolskis AR Borucki WJ (1996a) Influence of Jovian Extrasolar Planets on Transits of Inner Planets. In: AAS/Division for Planetary Sciences Meeting Abstracts #28, Bulletin of the American Astronomical Society, vol 28, p 1112

Dobrovolskis AR Borucki WJ (1996b) Influence of Jovian extrasolar planets on transits of inner planets. In: Bulletin of the American Astronomical Society, BAAS, vol 28, p 1112

Doyle LR, Carter JA, Fabrycky DC et al (2011) Kepler-16: A Transiting Circumbinary Planet. Science 333:1602, DOI 10.1126/science.1210923, 1109.3432

Eastman J, Siverd R Gaudi BS (2010) Achieving Better Than 1 Minute Accuracy in the Heliocentric and Barycentric Julian Dates. PASP122:935–946, DOI 10.1086/655938, 1005.4415

Fabrycky DC, Ford EB, Steffen JH et al (2012) Transit Timing Observations from Kepler. IV. Confirmation of Four Multiple-planet Systems by Simple Physical Models. ApJ750:114, DOI 10.1088/0004-637X/750/2/114, 1201.5415

Ford EB, Rowe JF, Fabrycky DC et al (2011) Transit Timing Observations from Kepler. I. Statistical Analysis of the First Four Months. ApJS197:2, DOI 10.1088/0067-0049/197/1/2, 1102.0544

Ford EB, Fabrycky DC, Steffen JH et al (2012a) Transit Timing Observations from Kepler. II. Confirmation of Two Multiplanet Systems via a Non-parametric Correlation Analysis. ApJ750:113, DOI 10.1088/0004-637X/750/2/113, 1201.5409

Ford EB, Ragozzine D, Rowe JF et al (2012b) Transit Timing Observations from Kepler. V. Transit Timing Variation Candidates in the First Sixteen Months from Polynomial Models. ApJ756:185, DOI 10.1088/0004-637X/756/2/185, 1201.1892

Gibson NP, Aigrain S, Roberts S et al (2012) A Gaussian process framework for modelling instrumental systematics: application to transmission spectroscopy. MNRAS419:2683–2694, DOI 10.1111/j.1365-2966.2011.19915.x, 1109.3251

Hadden S Lithwick Y (2014) Densities and Eccentricities of 139 Kepler Planets from Transit Time Variations. ApJ787:80, DOI 10.1088/0004-637X/787/1/80, 1310.7942

Heyl JS Gladman BJ (2007) Using long-term transit timing to detect terrestrial planets. MNRAS377:1511–1519, DOI 10.1111/j.1365-2966.2007.11697.x, astro-ph/0610267

Holczer T, Mazeh T, Nachmani G et al (2016) Transit Timing Observations from Kepler. IX. Catalog of the Full Long-cadence Data Set. ApJS225:9, DOI 10.3847/0067-0049/225/1/9, 1606.01744

Holman MJ Murray NW (2005) The Use of Transit Timing to Detect Terrestrial-Mass Extrasolar Planets. Science 307:1288–1291, DOI 10.1126/science.1107822, astro-ph/0412028

Holman MJ, Fabrycky DC, Ragozzine D et al (2010) Kepler-9: A System of Multiple Planets Transiting a Sun-Like Star, Confirmed by Timing Variations. Science 330:51, DOI 10.1126/science.1195778

Ioannidis P, Huber KF Schmitt JHMM (2016) How do starspots influence the transit timing variations of exoplanets? Simulations of individual and consecutive transits. A&A585:A72, DOI 10.1051/0004-6361/201527184, 1510.03276

Jontof-Hutter D, Ford EB, Rowe JF et al (2016) Secure Mass Measurements from Transit Timing: 10 Kepler Exoplanets between 3 and 8 $M_\oplus$ with Diverse Densities and Incident Fluxes. ApJ820:39, DOI 10.3847/0004-637X/820/1/39, 1512.02003

Kipping DM (2014) Characterizing distant worlds with asterodensity profiling. MNRAS440:2164–2184, DOI 10.1093/mnras/stu318, 1311.1170

Kostov VB, McCullough PR, Hinse TC et al (2013) A Gas Giant Circumbinary Planet Transiting the F Star Primary of the Eclipsing Binary Star KIC 4862625 and the Independent Discovery and Characterization of the Two Transiting Planets in the Kepler-47 System. ApJ770:52, DOI 10.1088/0004-637X/770/1/52, 1210.3850

Kostov VB, McCullough PR, Carter JA et al (2014) Kepler-413b: A Slightly Misaligned, Neptune-size Transiting Circumbinary Planet. ApJ784:14, DOI 10.1088/0004-637X/784/1/14, 1401.7275

Laughlin G Chambers JE (2001) Short-Term Dynamical Interactions among Extrasolar Planets. ApJ551:L109–L113, DOI 10.1086/319847, astro-ph/0101423

Le Verrier UJ (1877) Tables du mouvement de Neptune fondees sur la comparaison de la theorie avec les observations. Annales de l'Observatoire de Paris 14:1

Lithwick Y, Xie J Wu Y (2012) Extracting Planet Mass and Eccentricity from TTV Data. ApJ761:122, DOI 10.1088/0004-637X/761/2/122, 1207.4192

Martin DV (2017) Circumbinary planets - II. When transits come and go. MNRAS465:3235–3253, DOI 10.1093/mnras/stw2851, 1611.00526

Mayer P (1971) Eclipsing variable IU Aurigae. Bulletin of the Astronomical Institutes of Czechoslovakia 22:168

Mazeh T, Nachmani G, Holczer T et al (2013) Transit Timing Observations from Kepler. VIII. Catalog of Transit Timing Measurements of the First Twelve Quarters. ApJS208:16, DOI 10.1088/0067-0049/208/2/16, 1301.5499

Mills SM Fabrycky DC (2017) Kepler-108: A mutually inclined giant planet system. The Astronomical Journal 153(1):45, URL http://stacks.iop.org/1538-3881/153/i=1/a=45

Mills SM, Fabrycky DC, Migaszewski C et al (2016) A resonant chain of four transiting, sub-Neptune planets. Nature533:509–512, DOI 10.1038/nature17445

Miralda-Escudé J (2002) Orbital Perturbations of Transiting Planets: A Possible Method to Measure Stellar Quadrupoles and to Detect Earth-Mass Planets. ApJ564:1019–1023, DOI 10.1086/324279, astro-ph/0104034

Montet BT Johnson JA (2013) Model-independent Stellar and Planetary Masses from Multi-transiting Exoplanetary Systems. ApJ762:112, DOI 10.1088/0004-637X/762/2/112, 1211.4028

Nesvorný D Vokrouhlický D (2014) The Effect of Conjunctions on the Transit Timing Variations of Exoplanets. ApJ790:58, DOI 10.1088/0004-637X/790/1/58, 1405.7433

Nesvorný D Vokrouhlický D (2016) Dynamics and Transit Variations of Resonant Exoplanets. ApJ823:72, DOI 10.3847/0004-637X/823/2/72, 1603.07306

Nesvorný D, Kipping DM, Buchhave LA et al (2012) The Detection and Characterization of a Nontransiting Planet by Transit Timing Variations. Science 336:1133, DOI 10.1126/science.1221141, 1208.0942

Nesvorný D, Kipping D, Terrell D et al (2013) KOI-142, The King of Transit Variations, is a Pair of Planets near the 2:1 Resonance. ApJ777:3, DOI 10.1088/0004-637X/777/1/3, 1304.4283

Pál A Kocsis B (2008) Periastron precession measurements in transiting extrasolar planetary systems at the level of general relativity. MNRAS389:191–198, DOI 10.1111/j.1365-2966.2008.13512.x, 0806.0629

Price EM Rogers LA (2014) Transit Light Curves with Finite Integration Time: Fisher Information Analysis. ApJ794:92, DOI 10.1088/0004-637X/794/1/92, 1408.4124

Ragozzine D Wolf AS (2009) Probing the Interiors of very Hot Jupiters Using Transit Light Curves. ApJ698:1778–1794, DOI 10.1088/0004-637X/698/2/1778, 0807.2856

Schmitt JR, Agol E, Deck KM et al (2014) Planet Hunters. VII. Discovery of a New Low-mass, Low-density Planet (PH3 C) Orbiting Kepler-289 with Mass Measurements of Two Additional Planets (PH3 B and D). ApJ795:167, DOI 10.1088/0004-637X/795/2/167, 1410.8114

Schneider J (2003) Multi-planet system detection by transits. In: Combes F, Barret D, Contini T Pagani L (eds) SF2A-2003: Semaine de l'Astrophysique Francaise, p 149

Schneider J (2004) Multi-planet system detection with Eddington. In: Favata F, Aigrain S Wilson A (eds) Stellar Structure and Habitable Planet Finding, ESA Special Publication, vol 538, pp 407–410

Seager S Mallén-Ornelas G (2003) A Unique Solution of Planet and Star Parameters from an Extrasolar Planet Transit Light Curve. ApJ585:1038–1055, DOI 10.1086/346105, astro-ph/0206228

Steffen JH, Fabrycky DC, Ford EB et al (2012) Transit timing observations from Kepler - III. Confirmation of four multiple planet systems by a Fourier-domain study of anticorrelated transit timing variations. MNRAS421:2342–2354, DOI 10.1111/j.1365-2966.2012.20467.x, 1201.5412

Steffen JH, Fabrycky DC, Agol E et al (2013) Transit timing observations from Kepler - VII. Confirmation of 27 planets in 13 multiplanet systems via transit timing variations and orbital stability. MNRAS428:1077–1087, DOI 10.1093/mnras/sts090, 1208.3499

Ulrich RK (1986) Determination of stellar ages from asteroseismology. ApJ306:L37–L40, DOI 10.1086/184700

Welsh WF, Orosz JA, Carter JA et al (2012) Transiting circumbinary planets Kepler-34 b and Kepler-35 b. Nature481:475–479, DOI 10.1038/nature10768, 1204.3955

Wilson C (1985) The Great Inequality of Jupiter and Saturn: from Kepler to Laplace. Archive for History of Exact Sciences 33:15–290

Xie JW (2013) Transit Timing Variation of Near-resonance Planetary Pairs: Confirmation of 12 Multiple-planet Systems. ApJS208:22, DOI 10.1088/0067-0049/208/2/22, 1208.3312

Xie JW (2014) Transit Timing Variation of Near-resonance Planetary Pairs. II. Confirmation of 30 Planets in 15 Multiple-planet Systems. ApJS210:25, DOI 10.1088/0067-0049/210/2/25, 1309.2329